KSCE Journal of Civil Engineering (2014) 18(1):113-123

DOI 10.1007/s12205-013-0300-6

Geotechnical Engineering

pISSN 1226-7988, eISSN 1976-3808
www.springer.com/12205

Analysis on the Progressive Failure Process of Backfill Soil under Seismic Loads

H. Q. Yang* and D. Huang**

Received June 15, 2012/Revised November 27, 2012/Accepted February 20, 2013/Published Online November 1, 2013

Abstract

Knowledge of earth pressure and failure behavior of backfill soil is important to the design of retaining wall, especially in earthquake-prone region. However, most common methods, such as the Mononobe-Okabe method, only consider the equilibrium of forces, and ignore the failure behavior of backfill soil. To research the seismic response of soil-wall interaction system, the current study proposes an approximate analysis model based on three methods which are the pseudo-dynamic method, free field solution, and Mohr-Coulomb criterion. In this new model, the assumption about the shape of slip surface is not needed any more. The time-dependent earth pressure which depends on the motion pattern of the retaining wall is derived on the basis of fundamental solution of the free-field of backfill soil. Moreover, the evolution process of failure zone in backfill soil is determined by using the Melan's basic solution. Present analysis model is fit for different motion patterns of wall. In addition, earth pressure of both active and passive state can be determined by the present model. Through the simple numerical calculation, not only the time-dependent distribution of earth pressure, but also the visualized failure zone is obtained.

Keywords: *earth pressure, seismic, backfill soil, progressive failure*

1. Introduction

In severe earthquakes, foundations settle, retaining structures move and landslides occur. The seismic response of backfill soil can cause serious damage and large movement of structures (Ling *et al.*, 2001). In order to handle these problems, it is necessary to understand the failure mechanism of backfill soil under seismic loads and the earth pressure acting on the retaining wall.

Several classical methods to determine the seismic earth pressure have been developed. The pioneering work, which is named as pseudo-static approach, was firstly reported by Okabe (1924) and Mononobe and Matsuo (1929). This method is known as Mononobe-Okabe approach and is extensively used to calculate the dynamic earth pressure acting on the retaining wall all over the world. For pseudo-static, only force equilibrium is used and therefore the slip surface is assumed to be a straight line. Choudhury and Singh (2006b) provided the data related to active earth pressure by using pseudo-static analysis. In pseudo-static analysis, the dynamic loading induced by an earthquake is considered as time-independent, which ultimately assumes that the magnitude and phase of acceleration are uniform throughout the backfill. Apart from this, pseudo-static analysis does not consider the amplification of vibration which generally takes place near the ground surface and depends on various soil properties such as damping, elastic modulus, and shear modulus. To deal with these problems, Steedman (1990) and Choudhury (2006a) used a pseudo dynamic approach to predict the seismic response of a retaining wall. Ghosh (2007) extended the pseudo dynamic approach to consider the inclination of retaining wall in the evaluation of seismic passive earth pressure. However, both pseudo static and dynamic approach are based on the limit equilibrium theory without considering the deformation and failure behavior of soil and wall. Thus, these two kinds of approach need to assume an appropriate slip surface first.

An alternate analysis method for soil-structure interaction is to model the retaining wall by springs. The earth pressure is directly related to the displacement of the soil-structure interface and the stiffness of the springs. The soil-wall system examined in Scott's work (1973) is a semi-infinite uniform layer of viscoelastic material that is free at its upper surface, is bonded to a nondeformable rigid base, and is retained along one of its vertical boundaries by a rigid wall. Veletsos and Younan (1994) improved Scott's approach and proposed comprehensive numerical solutions for harmonic and transient excitations. However, these methods ignored the failure of backfill soil, and it may cause unsafe factors for the design of retaining wall (Christos *et al*., 2011). Rowland Richards (1999) established a simple kinematic model to predict the seismic earth pressure against retaining wall, in which plastic behavior of soil is included in the retaining wall analysis for the first time. Bathurst *et al.* (1988, 1992) has carried out a carefully monitored 3 m high models of geogrid reinforced soil walls. Through the

*Assistant Professor, School of Civil Engineering, Chongqing University, Chongqing 400030, China (Corresponding Author, E-mail: yanghaiqing06@163.com)
**Associate Professor, School of Civil Engineering, Chongqing University, Chongqing 400030, China (E-mail: hdcqy@yahoo.com.cn)

tests, the failure behavior of reinforced soil wall system are obtained. Meanwhile, a finite element program (GEOFEM) has been developed to meet the requirements of experimental model.

It is acceptable that the earth pressure depends on the movement of wall under seismic loads. Accordingly, the movement of wall depends on the exerted pressures behind the wall. Hence, there exists a very close relationship between earth pressure and the displacement of wall. In general, this interaction may usually be addressed with numerical simulations or dynamic interaction methods. However, owing to the complex expressions, it is not convenient for engineering application. Sometimes, these methods even need some material parameters which are not common.

In this paper, we proposed an approximate analysis approach to determine the earth pressure against the retaining wall and failure zone in backfill soil. By combining the pseudo dynamic method and free field solution, we established an analysis model of the earth pressure which depends on the motion pattern of the retaining wall. Moreover, the evolution process of failure zone in backfill soil is determined by using Melan's basic solution. At last, both the earth pressure and the visualized failure zone are obtained.

2. Analytical Model for the Failure Process of Backfill Soil under Seismic Loads

In this section, we follow the method and terminology used by Rowland *et al.* (1999). The backfill soil is a semi-infinite homogeneous material of density ρ_s. The upper surface of backfill soil is free, while its bottom is bonded to a rigid base. The backfill soil is initially retained on its vertical boundary by a rectangle retaining wall. The retaining wall is rigid and inflexural. Both fixed and movable retaining wall can be considered in present model. The height of the retaining wall and the backfill stratum are considered to be the same and denoted by H, as shown in Fig. 1. In present model, the backfill soil is simplified as an elastic-plastic material, which obeys the Mohr-Coulomb yield criterion. δ represents the friction coefficient on the interface between wall and soil.

Under seismic loads, deformation of the backfill soil will appear. If the retaining wall has the same displacement as that of backfill soil in the free field, the stress field of backfill soil will be the same as that in the free field too. Meanwhile, the earth pressure acting on the retaining wall does not exist. So, in order to obtain the failure zone, the deformation difference between the backfill soil and retaining wall should be determined first.

In this section, we will derive the free field analysis solution of backfill soil by using the pseudo dynamic method. Then, three different motion patterns of retaining wall are taken into account, earth pressure acting on the retaining wall is determined.

2.1 Free Field Analysis Solution of Backfill Soil based on the Pseudo Dynamic Method

According to the pseudo dynamic approach which considers finite shear wave velocity within the backfill material as proposed by Steedman and Zeng (1990), it is assumed that the phase and magnitude of both horizontal and vertical accelerations are varying along the height of the retaining wall. That is to say the acceleration is varied with time, depth and phase difference within the backfill.

According to pseudo dynamic method, the base of the wall is subjected harmonic horizontal and vertical seismic acceleration, which are a_h and a_v respectively. The acceleration at any depth z and time t can be expressed as:

$$a_h = k_h g \sin \omega\left(t - \frac{H-z}{V_s}\right) \tag{1a}$$

$$a_v = k_v g \sin \omega\left(t - \frac{H-z}{V_p}\right) \tag{1b}$$

where, k_h and k_v are horizontal and vertical seismic coefficients respectively. ω is the angular frequency. As already known, circular cyclic frequency ω of the harmonic vibration components under a seismic excitation can usually fluctuate between approximately 0 and 100 rad/s. V_s and V_p are shear wave and primary wave velocities in the backfill material respectively. t corresponds to time. H and z represent height as shown in Fig. 1. g is the acceleration of gravity.

Considering an homogeneous horizontal layer of backfill soil of infinite lateral extent with unit weight γ, the two dimensional equilibrium equations is given by:

$$\frac{\partial \sigma_x}{\partial x} + \frac{\partial \tau_{xz}}{\partial z} = -a_h \rho_s \tag{2a}$$

$$\frac{\partial \tau_{xz}}{\partial x} + \frac{\partial \sigma_z}{\partial z} = \gamma - a_v \rho_s \tag{2b}$$

where, x and z is shown in Fig. 1. ρ_s corresponds to density of backfill soil. σ_z, σ_x and τ_{xz} are stress field of backfill soil.

For the plane strain problem, the two dimensional strain and displacement relations are:

$$\varepsilon_x = -\frac{\partial u}{\partial x};\ \varepsilon_z = -\frac{\partial v}{\partial x};\ \frac{\gamma_{xz}}{2} = -\frac{1}{2}\left(\frac{\partial v}{\partial x} + \frac{\partial u}{\partial z}\right) \tag{3}$$

where, normal strain is positive in compressive zone. u and v are vertical and horizontal displacement of backfill soil.

According to the research of Rowland *et al.* (1999), the relation between rotation and displacements can be expressed as:

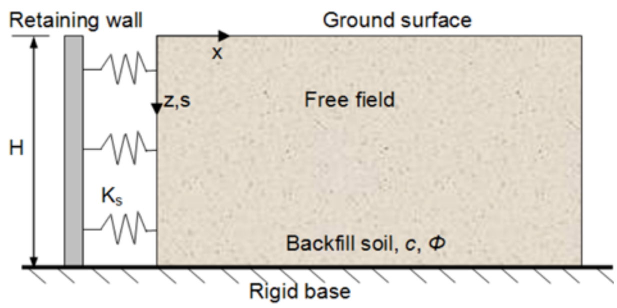

Fig. 1. Model for Analyzing the Interaction between Wall and Soil

$$\frac{\omega_{xz}}{2} = -\frac{1}{2}\left(\frac{\partial u}{\partial z} - \frac{\partial v}{\partial x}\right) \tag{4}$$

Therefore, the horizontal and vertical displacement can be expressed as:

$$u = \int \frac{\partial u}{\partial x}dx + \int \frac{\partial u}{\partial z}dz = -\int \varepsilon_x dx + \int \frac{1}{2}(\gamma_{xz} + \omega_{xz})dz \tag{5a}$$

$$v = \int \frac{\partial v}{\partial x}dx + \int \frac{\partial v}{\partial z}dz = -\int \frac{1}{2}(\gamma_{xz} - \omega_{xz})dz + \int \varepsilon_z dz \tag{5b}$$

However, for a half-space problem, all stress, strain and displacement components of soil in the present research are considered to be independent on the x coordinate, and only vary with z. Thus, this free-field problem can be simplified into a one-dimensional problem. The equilibrium equations can be solved directly by numerical integration. Considering the boundary condition on the top of backfill soil, the stress components can be defined as:

$$\tau_{xz} = -a_h \rho_s z \tag{6a}$$

$$\sigma_z = z(\gamma - \rho_s a_v) \tag{6b}$$

According to the equilibrium equations, the horizontal stress only conforms to the function of z, or just be a constant. In soil mechanics, it is usually expressed as a lateral earth pressure coefficient K times the vertical stress. For the initial static condition, the lateral earth pressure coefficient K for granular soil in the elastic state is often taken as (Rowland *et al.*, 1999):

$$\sigma_y = \sigma_x = K\sigma_z = (1 - \sin\phi)\sigma_z \tag{7}$$

where, ϕ is the internal friction angle of backfill soil.

Moreover, under this assumption, it can be concluded from Eqs. (3) and (4) that the value of rotation displacement ω_{xz} is equal to the shear strain γ_{xz}.

If soil is simply assumed as a linear elastic material before failure, the general relationship between stress and strain components are expressed by the general Hooke's law.

$$\varepsilon_x = \frac{1}{E}[\sigma_x - v_0(\sigma_y + \sigma_x)];\ \varepsilon_z = \frac{1}{E}[\sigma_z - v_0(\sigma_x + \sigma_y)];\ \gamma_{xz} = \frac{\tau_{xz}}{G} \tag{8}$$

The Young's modulus of soil is supposed to vary with the depth, it can be written as follows:

$$E = E_0\left(\frac{z}{H}\right);\ G = \frac{E}{2(1+v_0)} \tag{9}$$

Combining Eqs. (6)-(8), the strain field of soil can be obtained.

$$\varepsilon_x = \frac{z(\gamma - \rho_s a_v)}{E}(K - Kv_0 - v_0) \tag{10}$$

$$\varepsilon_z = \frac{z(\gamma - \rho_s a_v)}{E}(1 - 2Kv_0) \tag{11}$$

$$\gamma_{xz} = \frac{-a_h \rho_s z}{G} \tag{12}$$

Substituting Eqs. (10)-(12) into Eq. (5), we have:

$$u_s = \int \gamma_{xz} dz = \frac{2gH}{E_0 \omega}\rho_s k_h (1 + v_0) v_s \cos\left[\frac{\omega(z - H + tv_s)}{v_s}\right] \tag{13}$$

2.2 Earth Pressure Acting on the Wall

It is obvious that the distribution of earth pressure depends on the motion pattern of retaining wall. In order to obtain the earth pressure, the displacement of wall should be determined first. For rotation about the top of the wall (RT), rotation about the bottom of the wall (RB), and lateral translation (T), the wall displacements are:

$$\text{RT: } u_w = u_{w\max}(z/H)\text{ ; T: } u_w = u_{w\max}\text{ ;}$$
$$\text{RB: } u_w = u_{w\max}(1 - z/H)\text{ ;} \tag{14}$$

where $u_{w\max}$ is the maximum displacement corresponding to the three different motion patterns.

The total horizontal stress p acting on the wall is the sum of horizontal stress σ_s in the free field and the stress increment $\Delta\sigma_x$ due to the relative displacement between the wall and the soil in the free field.

$$p = \sigma_s + \Delta\sigma_x \tag{15}$$

The horizontal normal stress increment, $\Delta\sigma_x$, can be expressed as:

$$\Delta\sigma_x = K_s(u_s - u_w) \tag{16}$$

where K_s is the subgrade modulus of the backfill soil, u_s and u_w are the displacement of backfill soil and retaining wall respectively.

According to the works of Scott (1973), the subgrade modulus can be defined as:

$$K_s = CG/H \tag{17}$$

where C lumps all the geometric variables to modify the scale factor H into one average coefficient. In most cases, a value of C=1.35 seems appropriate based on finite element analysis (Huang, 1996). G represents the shear modulus of backfill soil.

It is well known that the distribution of earth pressure varies with the motion pattern of retaining wall. Taking rotation about the bottom of the wall (RB) for example, the distribution of earth pressure is determined as:

$$p(s) = (1 - \sin\phi)(\gamma - \gamma a_v)s + K_s\left\{\frac{2gH}{E_o \omega}\rho_s v_s k_h (1 + v_0)\right.$$
$$\left.\cos\left[\frac{\omega(s - H + tv_s)}{v_s}\right] - u_{w\max}(1 - s/H)\right\} \tag{18}$$

It should be noticed that Eq. (18) can be used for both active and passive states. Unlike traditional methods, the earth pressure obtained here is a general expression. Thus, this equation is suit to analyze the failure process of backfill soil, which may experience both active and passive states during earthquake.

The total horizontal thrust against the wall, N_E, can be calculated by integrating the horizontal stress along the height of the wall:

$$N_E = \int_0^H p(s)ds \tag{19}$$

The moment of the lateral earth pressure, M_E, about the base of the wall at the heel is:

$$M_E = \int_0^H (H-s)p(s)ds \tag{20}$$

So the distance or the height of the resultant force from the base of the wall, h_0, is:

$$h_0 = M_E/N_E \tag{21}$$

The shear force on the wall, T_E, is considered separately in the analysis and is determined by the knowledge of the wall frictional angle δ, such as $T_E = N_E \tan\delta$.

2.3 Approximate Stress Field of Backfill Soil

Owing to the harmonic equation of acceleration, it is not easy to obtain the stress field of backfill soil. Referring to the Melan's solution (Poulous *et al.*, 1974), the solution of stress field induced by strip loading is simplified as Fig. 2. According to Melan's assumption, the horizontal strip loads should be uniform along the whole height of wall. However, according to Eq. (18), the horizontal stress would be nonlinear along the height of backfill soil. It is not easy to integrate horizontal stress directly. Thus, we should adopt numerical method instead. Firstly, the horizontal stress $p(s)$ is divided into many sections, the distribution can be assumed to be uniform in each section. Then, the stress field induced by each section can be obtained by using Melan's basic solution. Finally, the stress distribution of stress in each point of backfill soil can be determined by summing up the solutions of all sections.

According to Melan's works, the basic solution of stress distribution resulted under the horizontal strip loads can be expressed as (Poulous *et al.*, 1974):

$$\sigma_{xp} = \frac{p(s)x}{2\pi(1-v_0)}\left\{\frac{x^2}{r_1^4} + \frac{x^2+8sz+6s^2}{r_2^4} + \frac{8sz(s+z)^2}{r_2^6} + \frac{1-2v_0}{2}\left[\frac{1}{r_1^2}+\frac{3}{r_2^2}-\frac{4z(s+z)}{r_2^2}\right]\right\} \tag{22}$$

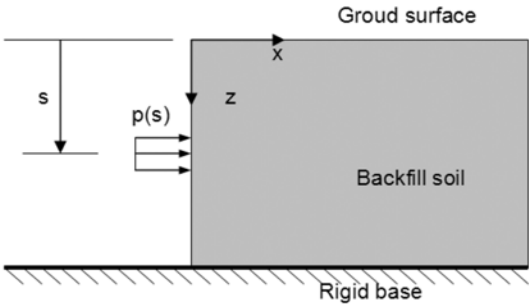

Fig. 2. Horizontal Equal Strip Loading Problem

$$\sigma_{zp} = \frac{p(s)x}{2\pi(1-v_0)}\left\{\frac{(z-s)^2}{r_1^4} - \frac{s^2+z^2+6sz}{r_2^4} + \frac{8szx^2}{r_2^6} - \frac{1-2v_0}{2}\left[\frac{1}{r_1^2} - \frac{1}{r_2^2} - \frac{4z(s+z)}{r_2^4}\right]\right\} \tag{23}$$

$$\tau_{xzp} = \frac{p(s)}{2\pi(1-v_0)}\left\{\frac{(z-s)x^2}{r_1^4} + \frac{(2sz+x^2)(s+z)}{r_2^4} - \frac{8sz(s+z)x^2}{r_2^6} + \frac{1-2v_0}{2}\left[\frac{z-s}{r_1^2} + \frac{3z+s}{r_2^2} - \frac{4z(s+z)^2}{r_2^4}\right]\right\} \tag{24}$$

where, s is the distance from the top of retaining wall to the point in the backfill soil, $r_1 = \sqrt{x^2+(z-s)^2}$; $r_2 = \sqrt{x^2+(z+s)^2}$.

The stress field of backfill soil can be obtained by integrating Eqs. (22) and (23).

$$\sigma_{xs} = \int_0^H \sigma_{xp}(s)ds \tag{25}$$

$$\sigma_{zs} = \int_0^H \sigma_{zp}(s)ds \tag{26}$$

$$\tau_{xzs} = \int_0^H \tau_{xzp}(s)ds \tag{27}$$

It is difficult to integrate Eqs. (25)~(27) directly. Numerical integrating should be adopted. In this paper, classical Newton integrating is used. The final stress field of backfill is determined as numerical solution.

2.4 Determine the Failure Zone in the Backfill Soil Behind Retaining Wall

In this paper, the classical Mohr-Coloumb criterion is adopted. The Mohr-Coloumb failure criterion can be expressed as:

$$\sigma_1 = \frac{2\cos\phi}{1-\sin\phi} + \sigma_3\frac{1+\sin\phi}{1-\sin\phi} \tag{28a}$$

$$\sigma_1 = \frac{\sigma_{xp}+\sigma_{zp}}{2} + \sqrt{\left(\frac{\sigma_{xp}+\sigma_{zp}}{2}\right)^2 + \tau_{xzp}^2}\,;$$

$$\sigma_3 = \frac{\sigma_{xp}+\sigma_{zp}}{2} - \sqrt{\left(\frac{\sigma_{xp}+\sigma_{zp}}{2}\right)^2 + \tau_{xzp}^2} \tag{28b}$$

where, c is the cohesion of backfill soil.

In order to determine the failure zone in backfill soil, the backfill soil is divided into many small rectangle zones with the same size. Then, the stress field in each small rectangle is represented by the stress at the center point. The stress components at each center point are defined by Eqs. (25~27). Finally, the stress components are substituted into Eq. (28). When the maximum principal stress defined in Eq. (28b) is bigger than the one expressed in Eq. (28a), the rectangle zone is defined as a failure zone.

3. Results and Discussion

In order to illustrate the performance of the present model, sensitive analysis of parameters is shown in this section. The progressive failure model for backfill soil described in Section 2 has been implemented in a simple Matlab code.

The following parameters are considered: $\phi = 18$ Deg., $c = 60$ kPa, $E_0 = 600$ MPa, $\nu_0 = 0.25$, $\delta = 20$ Deg., $\rho_s = 2000$ kg/m^3, $\omega = 32.14$ rad/s, H = 5.0 m, $k_h = 0.1$, $k_v = 0.1$, t = 0.02 s.

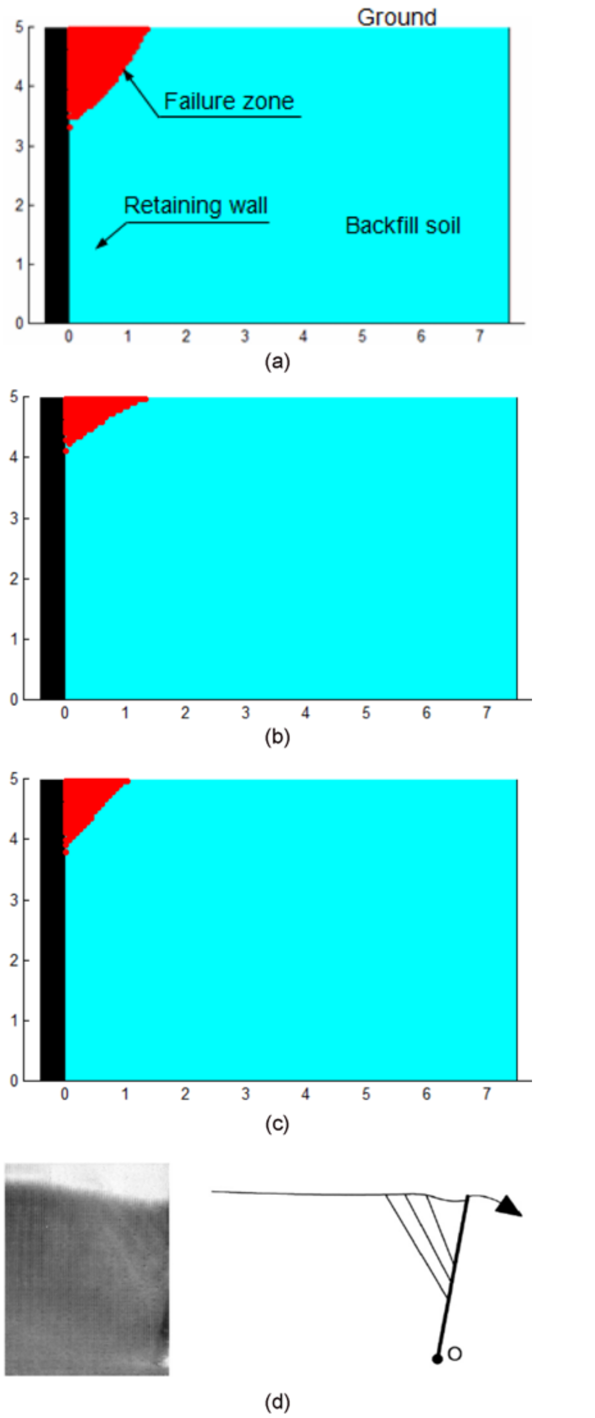

Fig. 3. Failure Model of Backfill Soil for Different Motion Patterns of Retaining Wall: (a) RB, (b) T, (c) RT, (d) Experimental Photo of Widulinki *et al.* (2011)

In this section, both the distribution of earth pressure and the range of failure zone are determined. Some special failure behaviors of backfill soil are analyzed as below.

3.1 Failure of Backfill Soil under Different Motion Patterns of Retaining Wall

The failure model of backfill soil at different motion patterns of retaining wall is shown as Fig. 3. In Fig. 3, the black rectangle represents retaining wall, and the blue zone is backfill soil behind the retaining wall. During the period of earthquake, part of the backfill soil will be failure which is depicted in red color. The units of both horizontal and vertical axis are meter. Three typical motion patterns of retaining wall of rotation about the top of the wall (RT), rotation about the bottom of the wall (RB), and lateral Translation (T) are considered here. In the examples shown in Fig. 3, only active displacement of the retaining walls is considered. Meanwhile, the maximum displacement is set to be the same. Then, comparison between different motion patterns is conducted as follows.

It can be seen from Fig. 3 that the slip surface in the backfill soil can be approximately considered as a straight line for the T and RT motion patterns, which is popularly adopted by traditional limit equilibrium methods. However, for the RB motion pattern, the slip surface is a curve, which can be simplified as the combination of a logarithmic spiral near the wall and a straight line in the planar shear zone near the ground. An obvious difference between present model and limit equilibrium methods is that the slip surface doesn't go through the bottom of retaining wall. This is common in engineering practice. Comparing with the experimental result of Widulinski (2011) as shown in Fig. 3(d), we find the slip surface do not always go through the bottom of retaining wall. The present model doesn't need to assume the slip surface, while the limit equilibrium methods are limited at this. So, it sounds more reasonable than the assumption of forming a failure line through the bottom of retaining wall.

Figure 4 shows the distribution of earth pressure acting on retaining wall for different motion patterns of retaining wall. When the maximum displacement $u_{w\,\max}$ of retaining wall is the same, the earth pressure for RT motion pattern is larger than the

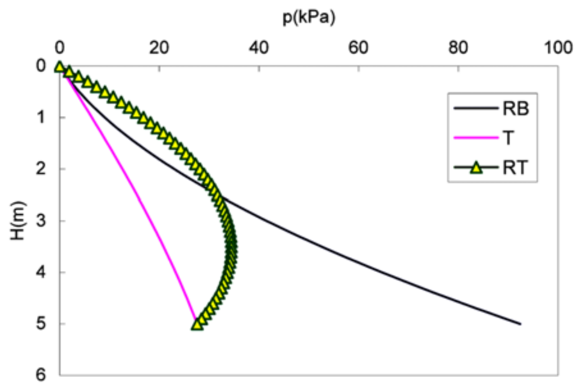

Fig. 4. Earth Pressure Behind Retaining Wall for Different Motion Patterns of Retaining Wall

T one. The largest earth pressure is the RB motion pattern, especially near the bottom of retaining wall.

3.2 Evolution of Failure Zone under Pseudo Dynamic Seismic Loads

During the period of earthquake, the acceleration is time-dependent. So the failure zone in the backfill soil will vary with time. In the following example, only RB motion pattern is taken into account, providing that the retaining wall moves against the backfill.

The evolution process of failure zone in backfill soil is depicted as Fig. 5. It is obvious that the range of failure zone expands with time. Moreover, the slip surface shifts from straight line to curve, which is the combination of logarithmic spiral and straight line.

Owing to the time dependence of seismic loads, the height of the resultant force acting on the retaining wall will change with time, as shown in Fig. 6. According to the Mononobe-Okabe (M-O) method, the height is assumed to be one third of the height of retaining wall, which is equal to 1.67 m for this example. However, the calculated maximum height of the height of the resultant force acting on is 1.55 m (<1.67 m), which is lower than the Mononobe-Okabe method. The reason for this is that the top part of backfill soil is failure and exits to support the retaining wall for present motion pattern, so the height becomes lower.

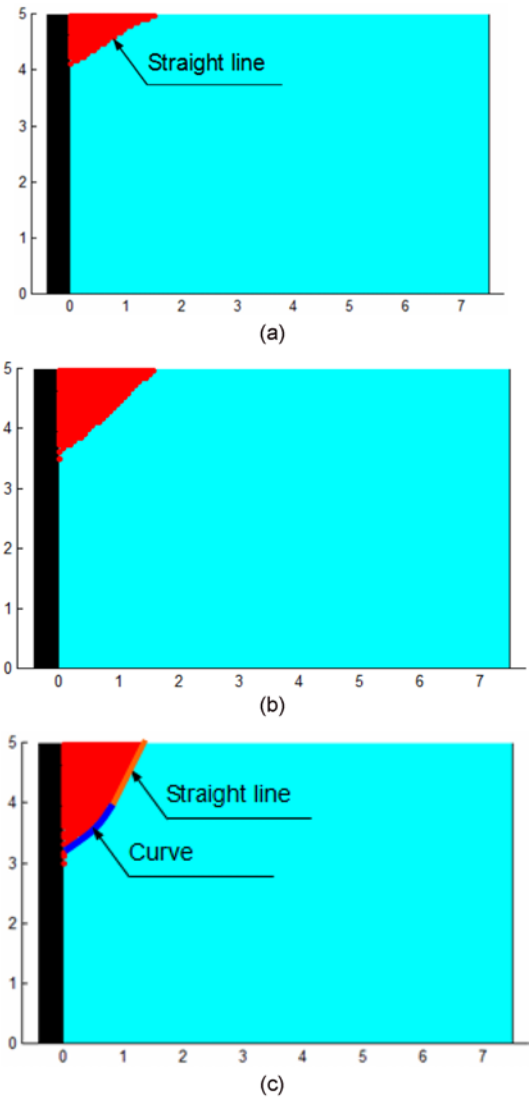

Fig. 5. Evolution of Failure Zone in Backfill Soil: (a) t = 0.1s, (b) t = 0.15s, (c) t = 0.2s

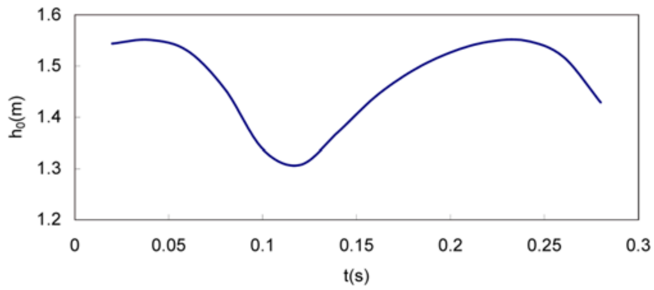

Fig. 6.The Height of the Resultant Force from the Base of the Wall

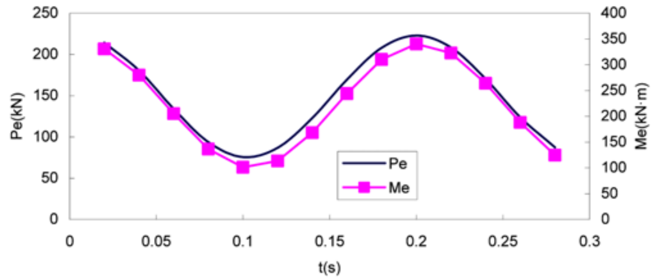

Fig. 7. The Total Horizontal Thrust and Moment Against the Wall

Figure 7 shows the total horizontal thrust and moment against the wall. The left vertical axis represents the total horizontal thrust, while the right one is the moment about the base of the wall at the heel. It is well known that M-O results are time-independent, while present one is time- dependent. The maximum value of resultant force P_e is close to the results obtained by M-O method (187.5 kN), merely with error by 6.25%.

3.3 Comparison of Failure Characters between Active, Static and Passive State

In present model, the distribution of earth pressure is related to the displacement of retaining wall. Three different states, which are active, static and passive ones, are considered respectively. Unlike the definition of limit equilibrium, the active, static and passive states which represent the direction of wall movement presented here are not the critical state of force equilibrium. In this model, they only represent the direction of wall movement. The positive displacement means that the wall moves against the backfill soil, while the negative displacement means that the wall moves toward the backfill soil.

The failure zones for RB motion pattern under active, static and passive states are depicted in Fig. 8. It can be seen from Fig. 8 that the extent of failure zone under passive state is maximum, especially in vertical direction. In addition, it is also indicated

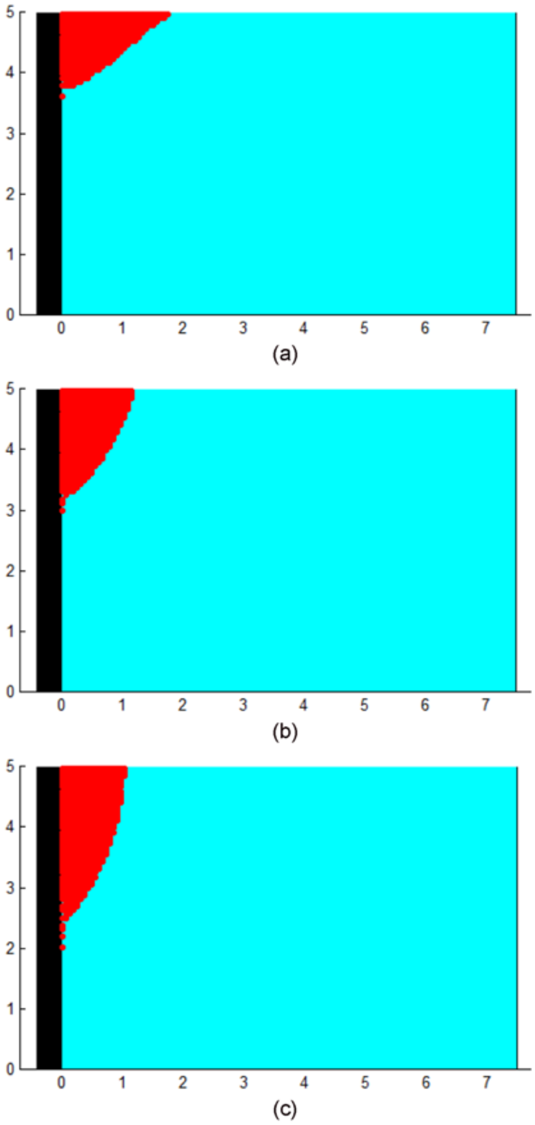

Fig. 8. Failure Characters for Active, Static and Passive States (RB Pattern): (a) Active State when $u_{w\,max} = 0.0005H$, (b) Static State when $u_{w\,max} = 0.0$, (c) Passive State when $u_{w\,max} = -0.0005H$

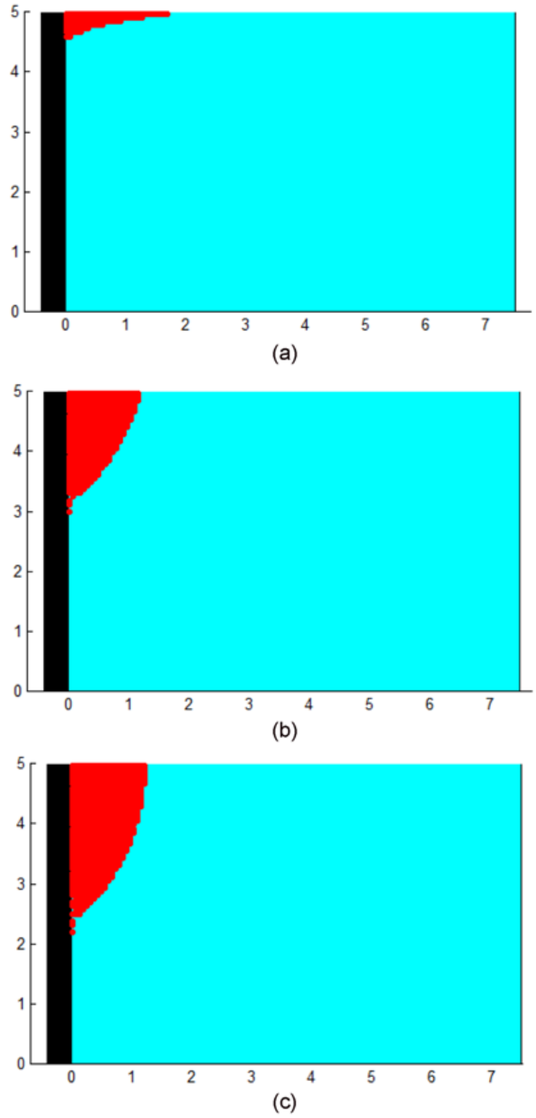

Fig. 9. Failure Characters for Active, Static and Passive State (T Pattern): (a) Active State when $u_{w\,max} = 0.00025H$, (b) Static State when $u_{w\,max} = 0.0$, (c) Passive State when $u_{w\,max} = -0.00025H$

that the assumption of logarithmic spiral slip surface is acceptable for RB motion pattern. This assumption is always adopted in the upper bound theorem of limit analysis. This shows good agreement with experimental results of Widulinski *et al.* (2011).

Similarly, the failure zones for RT and T motion pattern under active, static and passive states are described in Fig. 9 and Fig. 10. From Fig. 9 and Fig. 10, it can be concluded that the slip surface is nearly a straight line. For limit equilibrium method, the slip surface is frequently assumed as a straight line. It shows good agreement with present model for active state. However, in present model the slip surface become a curve under passive condition. So, it sounds unreasonable to assume the slip surface as a straight line under active condition.

The distribution of earth pressure, corresponding to Figs. 8~10, is shown in Fig. 11. It can be seen that the passive earth pressure is bigger than other two states. In addition, the distribution of earth pressure is not a triangle pattern, which is widely adopted in limit equilibrium methods, especially when the top part of backfill soil has been failure.

3.4 Effects of the Cohesion, Internal Frictional Angle and Horizontal Acceleration on the Failure Zone

Taking RB motion pattern for example, it is assumed that the retaining wall would move against the backfill soil, and the maximum displacement is the same for different parameters. Then, Sensitive analysis is conducted as follows.

Figure 12 shows the effects of horizontal acceleration on the failure zone. It is obvious that the failure zone is expanded as the

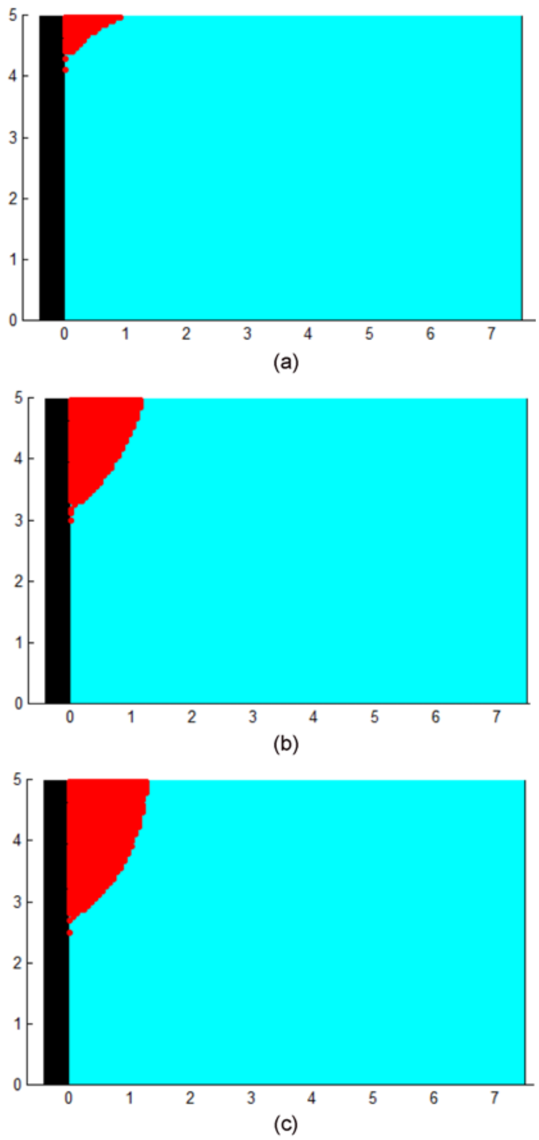

Fig. 10. Failure Characters for Active, Static and Passive State (RT Pattern): (a) Active State when $u_{w\,max}$ = -0.00025H, (b) Static State when $u_{w\,max}$ = 0.0, (c) Passive State when $u_{w\,max}$ = -0.00025H

horizontal acceleration increases. This has not been revealed by traditional method. Moreover, it is also indicated in Fig. 12 that the slip surface will change with the magnitude of seismic loads. However, most of published literatures think that the slip surface is fixed and pass through the bottom of retaining wall (Choudhury, 2006a; Mononobe, 1929; Steedman, 1990). However, the slip surface observed in the experiment of Widulinski (2011) don't go through the bottom of retaining wall. Thus, if we always assume the slip surface pass through bottom, it may cause unsafe factors of the retaining system.

Figure 13 shows the effects of cohesion of soil on the failure zone. It is obvious that the extent of failure zone increases with the cohesion of soil decreases. When the cohesion is zero, the failure zone is similar to the calculation model adopted in M-O

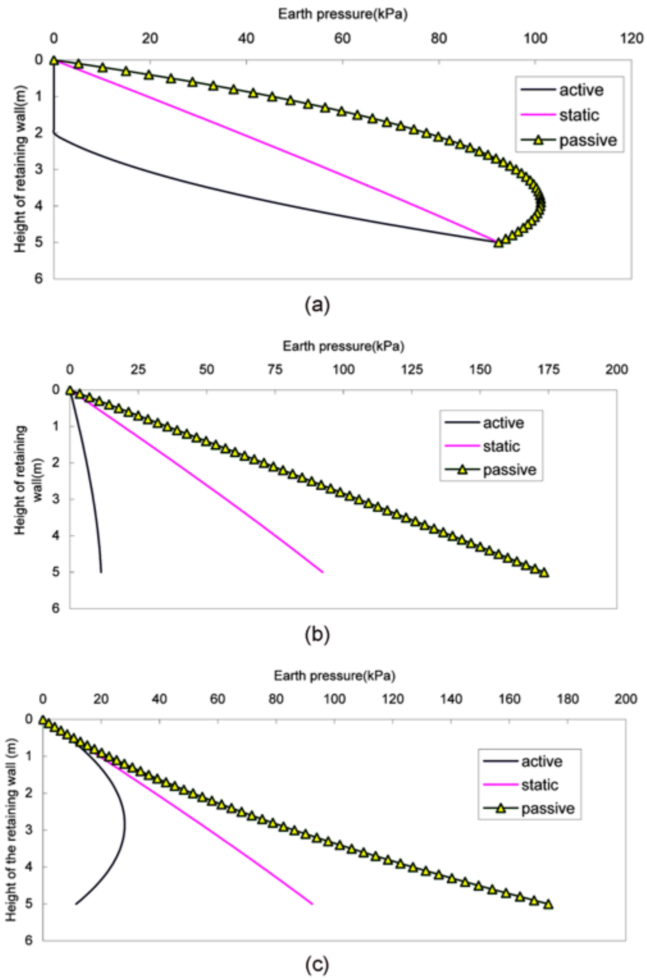

Fig. 11. Earth Pressure for Different Motion Patterns of Retaining Wall: (a) RB, (b) T, (c) RT

method, as shown in Fig. 13d. So, it can be said that M-O method is a special case of present model.

Figure 14 shows the effects of internal frictional angle of soil on the extent of failure zone. It can be seen from Fig. 14 that the internal frictional angle of soil has great effects on the appearance of failure zone, especially at the depth of slip surface.

Many efforts have been made in the past, for example, professor Richard Bathurst of RMC Canada and his former PhD student Magady made a shaking table test for wall reinforced with geogrid (Bathurst and Benjamin, 1990). In order to test present model, the results obtained by present model are compared with experimental results and other method. The experimental results come from Bathurst and Bengamin's (1990) work, as depicted in Fig. 15. The slip surfaces obtained by different methods are shown in Fig. 15. It can be concluded that present model show good agreement with experimental results. In addition, we also obtained a similar failure model as finite element method, as depicted in Fig. 16.

4. Conclusions

In this study, an approximate analysis model for the soil-wall

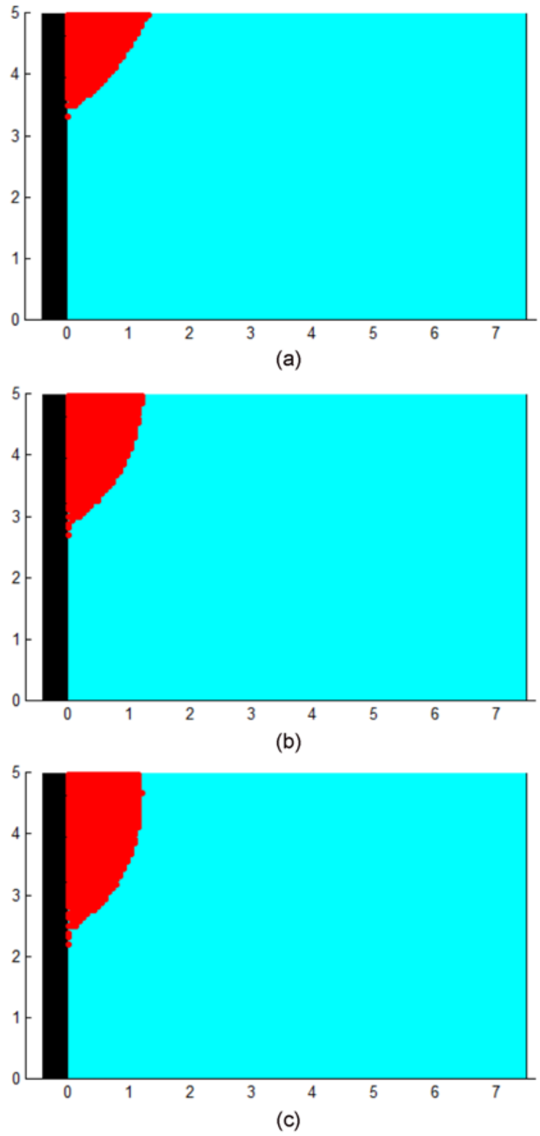

Fig. 12. Effects of Horizontal Acceleration on the Failure Zone: (a) k_h = 0.1, (b) k_h = 0.3, (c) k_h = 0.5

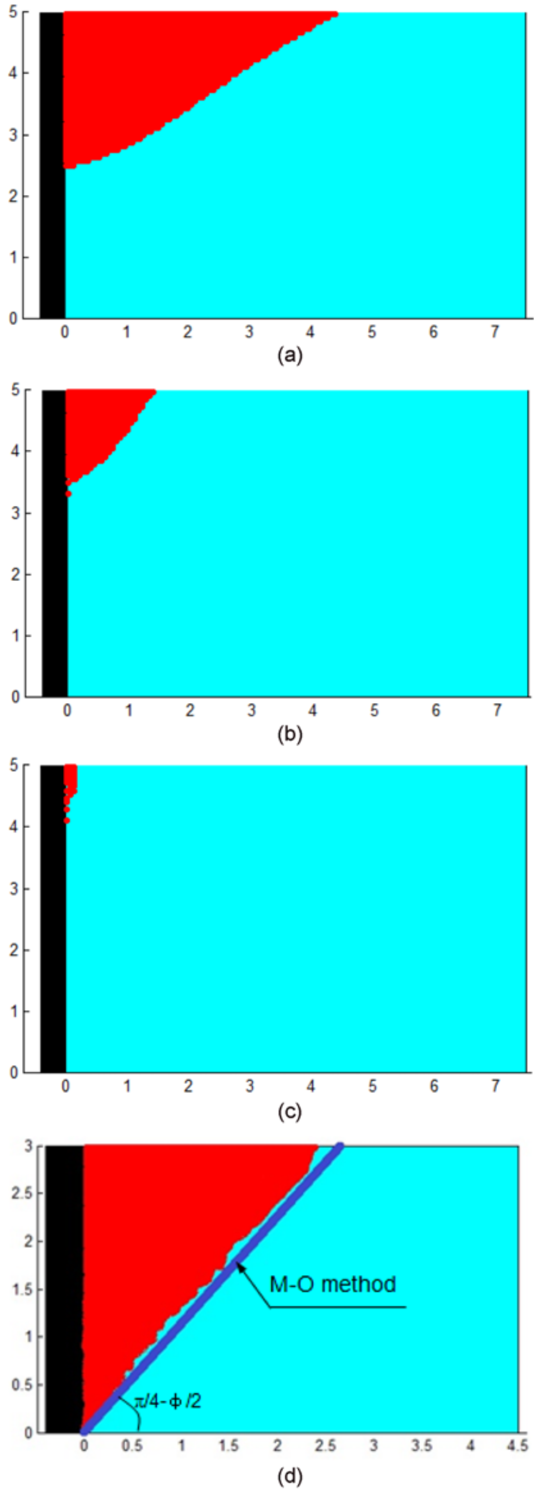

Fig. 13. Effects of Cohesion of Soil on the Failure Zone: (a) c = 40 kPa, (b) c = 60 kPa, (c) c = 80 kPa, (d) c = 0 kPa

system is established. The primary advantage is that it doesn't involve assumptions about the slip surface and the state of earth pressure. Furthermore, the new model takes the interaction between wall and backfill soil into account. The time-dependent evolution process is determined by a simple numerical calculation. Based on the new approach, the following remarks may be made:

Three typical motion patterns of retaining wall, including rotation about the top of the wall (RT), rotation about the bottom of the wall (RB), and lateral Translation (T), are considered here, respectively. When the maximum displacement $u_{w\,\max}$ of retaining wall is the same, the earth pressure for RT motion pattern is larger than the T one. The largest earth pressure is the RB motion pattern, especially near the bottom of retaining wall.

Moreover, an obvious difference between present model and limit equilibrium methods is that the slip surface doesn't always go through the bottom of retaining wall. This result sounds more reasonable in practical engineering.

For the passive state, the distribution of earth pressure is not a triangle pattern, which is widely adopted in limit equilibrium methods, especially when the top part of backfill soil has been

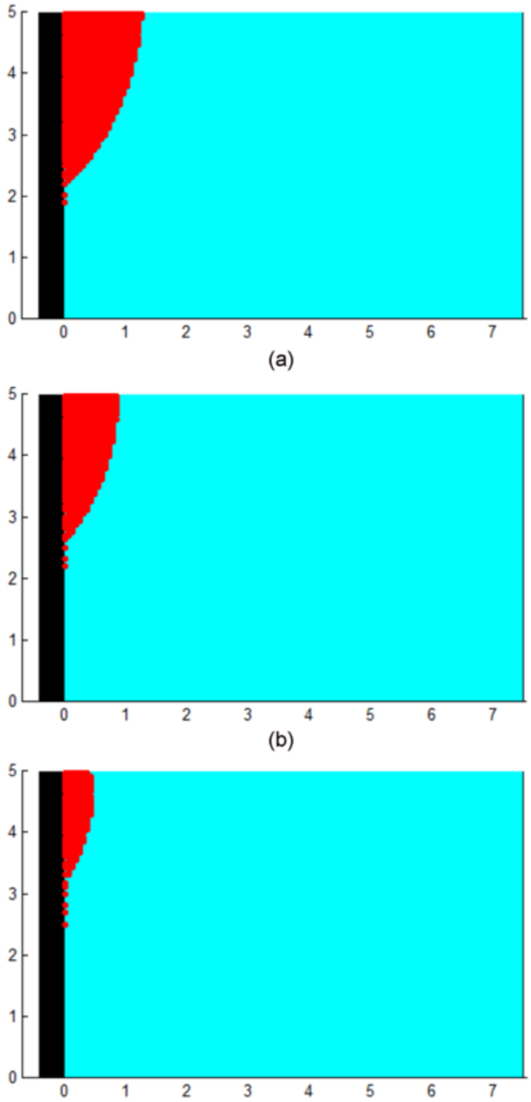

Fig. 14. Effects of Internal Frictional Angle of Soil on the Failure Zone: (a) ϕ=15 Deg., (b) ϕ=20 Deg., (c) ϕ=25 Deg.

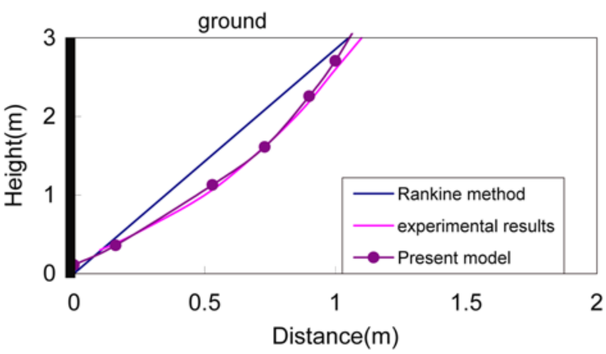

Fig. 15. Slip Surface Obtained by Different Methods

failure.

Moreover, it is also revealed that the slip surface will change with the magnitude of seismic loads. However, most of published literatures think that the slip surface is fixed.

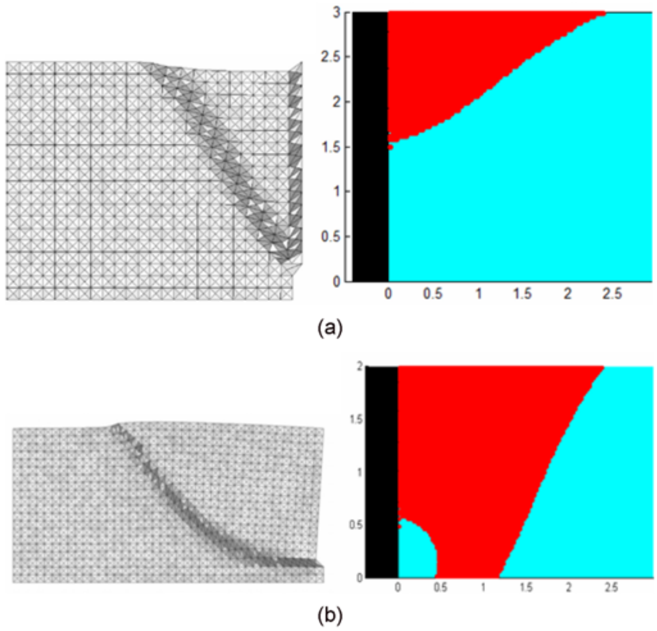

Fig. 16. Failure Models Obtained by Finite Element Method (Widulinski L, 2011) and Present Model: (a) Active State, (b) Passive State

Although the analytical model and results are limited to elastic materials, some of the conclusions are useful as they help identify soil-structure interaction mechanisms and evaluate the key parameters that determine the response of the backfill soil during seismic loading.

Acknowledgements

The work is supported by the Fundamental Research Funds for the Central Universities (Nos. CDJZR12205526, CDJZR13200039) and Specialized Research Fund for the Doctoral Program of Higher Education of China (No. 20120191120048).

References

Bathurst, R. J. and Benjamin, D. J. (1990). “Failure of a geogrid-reinforced soil wall.” *Transportation Research Record*, Vol. 18, pp. 109-116.

Bathurst, R. J., Benjamin, D. J., and Jarrett, P. M. (1988). “Laboratory study of geogrid reinforced soil walls.” *Geosynthetics for Soil Improvement*, ASCE Special Publication, Holtz, Ed., Vol. 18, pp. 178-192.

Bathurst, R. J., Karpurapu, R. G., and Jarrett, P. M. (1992). “Finite element analysis of a geogrid reinforced soil wall.” *ASCE Geotechnical Special Publication No. 30: Grouting, Soil Improvement and Geosynthetics*, Borden, Holtz, Juran, Ed., Vol. 2, pp. 1213-1224.

Choudhury, D. and Nimbalkar, S. (2006a). “Pseudo-dynamic approach of seismic active earth pressure behind retaining wall.” *J. Geotech. Geol. Eng.*, Vol. 24, No. 1, pp. 1103-1113.

Choudhury, D. and Singh, S. (2006b). “New approach for estimation of static and seismic active earth pressure.” *J. Geotech. Geol. Eng.*, Vol. 24, No. 1, pp. 117-127.

Christos, G. and George, M. (2011). “Interpretation of dynamic retaining wall model tests in light of elastic and plastic solution.” *Soil Dyn. Earthq. Eng.*, Vol. 31, No. 1, pp. 16-24.

Ghosh, P. (2007). “Seismic passive earth pressure behind non-vertical retaining wall using pseudo-dynamic analysis.” *J. Geotech. Geol. Eng.*, Vol. 25, No. 6, pp. 693-703.

Huang, C. J. (1996). *Plastic analysis for seismic stress and deformation fields*, PhD Thesis, Dept of Civ. Engrg., SUNY at Buffalo, Buffalo, N.Y., pp. 70-75.

Ling, H. I., Leshchinsky, D., and Chou, N. N. S. (1993). “Post-earthquake investigation on several geosynthetic-reinforced soil retaining walls and slopes during 1999 Ji-Ji earthquake of Taiwan.” *Soil Dyn. Earthq. Eng.*, Vol. 1, No. 4, pp. 297-313.

Mononobe, N. and Matsuo, H. (1929). “On the determination of earth pressure during earthquakes.” *Proc. of the World Engineering Conference*, Tokyo, Vol. 9, pp. 177-185.

Okabe, S. (1924). “General theory on earthquake pressure and seismicstability of retaining wall and dam.” *J. Jpn. Soc. Civil. Eng.*, Vol. 10, No. 5, pp. 1277-1323.

Poulous, H. G. and Davis, E. H. (1974). *Elastic solutions for soil and rock mechanics*, John Wiley & Sons, Incorporated, New York.

Rowland, R. J., Huang, C. J., and Fishman, K. L. (1999). “Seismic earth pressure on retaining structures.” *J. Geotech. Geoenviron. Eng.*, ASCE, Vol. 125, No. 9, pp. 771-778.

Scott, R. F. (1973). “Earthquake-induced pressures on retaining walls.” *Proc. of 5th World Conference on Earthquake Engineering*, Tokyo, pp. 1611-1620.

Steedman, R. S. and Zeng, X. (1990). “The influence of phase on the calculation of pseudo-static earth pressure on a retaining wall.” *Geotechnique*, Vol. 40, No. 1, pp. 103-112.

Veletsos, A. S. and Younan, A. H. (1994). “Dynamic modeling and response of soil-wall systems.” *J. Geotech. Engrg.*, ASCE, Vol. 120, No. 12, pp. 2155-2179.

Widulinski, L., Tejchman, J., Kozicki, J., and Lesniewska, D. (2011). “Discrete simulations of shear zone patterning in sand in earth pressure problems of a retaining wall.” *Int. J. Solids Struct.*, Vol. 48, Nos. 7-8, pp. 1191-1209.